

Structural specifics of laser welded joints of dissimilar steels

Artemii Bernatskyi¹, Mykola Sokolovskyi¹, Oleksandr Siora¹, Yurii Yurchenko¹, Nataliia Shamsutdinova^{1,2}, Oleksandr Danyleiko^{1,2}, Iryna Siora³

¹Department of Specialized High-Voltage Technique and Laser Welding, E.O. Paton Electric Welding Institute of the National Academy of Sciences of Ukraine, Kyiv, UKRAINE

²Department of Laser Systems and Advanced Technologies, E.O. Paton Educational and Research Institute of Material Science and Welding, National Technical University of Ukraine «Igor Sikorsky Kyiv Polytechnic Institute», Kyiv, UKRAINE

³Department of Surface Biomedical Problems Chuiko Institute of Surface Chemistry of the National Academy of Sciences of Ukraine, Kyiv, UKRAINE

Corresponding Author: Artemii Bernatskyi
E-mail: Bernatskyi@paton.kiev.ua

ABSTRACT: Modern trends in the reduction of weight, material intensity, as well as the cost of constructions in various branches of industry, such as transport and power engineering, the aerospace industry and others make it necessary to combine parts made of different materials into one. As such, a combination of stainless high-chromium steels with carbon or low-alloy steels is commonly found in designs of various industry branches, such as transport manufacturing, aerospace industry and power engineering. The purpose of this study is to investigate the specific features of the structure and mechanical characteristics of butt joints of stainless steels with carbon steels obtained via means of laser welding. Over the course of the study, two test samples were created and analyzed. As a result of the experiment, the characteristic features, inherent in the structures obtained during laser welding of AISI 304 and AISI 1010 steels are given. As the result the study of the structure and mechanical characteristics of welded joints of AISI 304 stainless steel and AISI 1010 carbon steel, it was established that optimal welded joints are formed when using such technological techniques as welding with a shift of a sharply focused laser beam relative to the joint line to the side of a high-chromium steel sample and using gas protection for both the melting bath and the cooling weld metal.

NOMENCLATURE

Symbol	Description	Unit
P	Laser radiation power	kW
V	Welding speed	mm/s
ΔF	Defocusing of the lens	mm
Q	Gas flow rate	l/s
$HV0.5$	Microhardness (Vickers)	MPa
σ_e	Temporary rupture resistance	MPa

Key words: stainless steel, carbon steel, butt welded joints, laser welding, structural features, strength of welded joints.

Date of Submission: 10-11-2023

Date of acceptance: 26-11-2023

I. INTRODUCTION

Modern trends in the reduction of weight, material intensity, as well as the cost of constructions in various branches of industry, such as transport and power engineering, the aerospace industry and others make it necessary to combine parts made of different materials into one [1]. Usually, different grades of steel are used for these purposes [2]. To connect such parts, the usage of welding technologies, that allow for obtaining of the welded joints, properties of which are not inferior to the properties of the joined materials is necessary [3]. To the greatest extent, these requirements are satisfied by welding technologies using concentrated energy flows – laser [4], electron beam, laser-arc [5]. However, the specifics of the formation of the weld seam during welding

of dissimilar metals, even using concentrated energy flows, lead to chemical and structural inhomogeneities of the metal, which negatively affect the further performance of the welded joint [6].

After carrying out a literary analysis of recent research studies in this regard, it was noted, that in welded assemblies of power plants and various chemical equipment, a combination of stainless high-chromium steels with carbon or low-alloy steels is commonly found [7]. At the same time, high-alloy steel is used only in the structural areas that are in direct contact with an aggressive environment. The main load-bearing part of the structure in such designs is commonly made of inexpensive pearlitic steel. The use of welded joints made of dissimilar steels allows to significantly reduce the consumption of high-alloyed steels, as well as to increase the load-bearing capacity and performance of the product [8].

At the same time it was noted that the specifics of welding dissimilar steels point out that in order to obtain high-quality and reliable welded joints in specific conditions, it is necessary to apply welding techniques that prevent the formation of cracks in the weld metal [9], exclude any changes of the chemical composition and structure of the welded metals in the fusion zone [10] (which otherwise would lead to the formation of structural inhomogeneity) and ensure the production of welded joints with the closest coefficients of linear expansion of the welded metals [1, 3, 7]. The structural heterogeneity, visible in the fusion zone of dissimilar steels, consists of a decarburized layer on the side of the less alloyed steel and a carburized layer on the side of the more alloyed steel [4, 6, 10]. These layers are formed thanks to the transfer of carbon between steels. The appearance of structural heterogeneity and the degree of its development are determined by the sum of the factors contributing to the transfer of carbon from a less alloyed metal to a more alloyed one [9]. The appearance of transitional structures in the fusion zone during welding of dissimilar steels is explained not only by the crystallization features of two alloys with different crystal lattices, but also by the conditions of fusion for materials of different compositions [10]. For this reason, an interlayer of transition composition is inevitable in the fusion zone on the side of the weld metal. Its width depends on the conditions of crystallization and lies within 0.2...0.8 mm. At the location of the intermediary layer, an austenite seam, growing to the border of the alloy, diluted with pearlitic (or carbon) steel is observed, as well as the resulting sharp decrease in the concentration of alloying austenite elements. Therefore, a brittle martensitic section is formed in the aforementioned intermediary layer, which can lead to the destruction of the fusion zone and decrease the operational reliability of the welded joint [6].

The purpose of this study is to investigate the specific features of the structure and mechanical characteristics of butt joints of stainless steels with carbon steels obtained via means of laser welding.

II. EXPERIMENTAL SETUP

To improve the characteristics of butt joints made of dissimilar steels, following basic technological methodics were developed and utilized: laser welding with a defocused beam; displacement of the sharply focused and defocused laser beam relative to the joint line; use of a substrate during welding; the use of various systems of gas protection of the welding bath. In order to determine the effectiveness of their application, a series of experiments was conducted for each of the listed methodics.

In the experiments, a Nd:YAG laser "DY-044" with a radiation power of up to 4.4 kW and a radiation wavelength of $\lambda=1.06 \mu\text{m}$, manufactured by the company "Rofin-Sinar" (Germany) was used. On a laboratory bench developed on the basis of a three-coordinate manipulator, experimental studies were carried out on laser welding of butt heterogeneous joints made of high-chromium stainless steel AISI 304 (1.5 mm thick) with carbon steel AISI 1010 (1.5 mm thick), which made it possible to establish the disadvantages and advantages of the following technological techniques. During the research, the technological parameters varied within the following limits: laser radiation power P: from 2.0 to 4.0 kW, welding speed V: from 33.0 to 100.0 mm/s, defocusing value ΔF : 0...-15 mm. Welding was carried out in an argon environment with flow rate (Q) varying from 0.1 to 0.2 l/s.

It has been established that from the point of view of the formation of the geometry of the seam and the absence of defects in the form of cracks, underwelds and burns, optimal welded joints are formed when using such basic technological techniques as welding with a sharply focused beam, when the laser beam is shifted to the side of the high-chromium steel sample relative to the joint line, as well as using gas protection both for the welding bath and for the cooling metal of the weld.

Analytical scanning electron microscopy was used to study the general nature of the distribution of chemical elements in the studied area and to determine the chemical composition in local areas, for example, in the area of phase separations and segregation in welded joints made of AISI 304 and AISI 1010 steels. The research was carried out using "Philips SEM-515" scanning electron microscope, equipped with the "LINK" energy dispersive spectrometer.

III. RESULTS AND DISCUSSION

Over the course of the study, two test samples were welded, respectively, No. 1, with the laser beam moving along the joint line and No. 3 with an laser beam offset of 0.7 mm from the joint line to the AISI 304 side of the joint at the following modes: defocusing of the lens $\Delta F = 0$ mm, argon consumption $Q = 0.1$ l/s, welding speed $V = 40$ mm/s, laser radiation power $P = 2.0$ kW. As a result of the experiment, the characteristic features, inherent in the structures obtained during laser welding of AISI 304 and AISI 1010 steels are given.

In the No. 1 sample, the weld seam has a clearly expressed crystalline structure, which is presented in the form of crystallites, that present themselves by the characteristic columnar shape. Crystallites are oriented from the fusion line in the direction of the center of the seam, with dimensions $h \times l$ varying from $5 \dots 10 \mu\text{m}$ to $10 \dots 75 \mu\text{m}$, as well as $HV0.5 = 5430 \dots 5540$ MPa microhardness (Fig. 1, a-d).

In the fusion line with AISI 1010, the size of the weld metal crystallites increases to $10 \dots 150 \mu\text{m}$, while the microhardness decreases, averaging around $HV0.5 = 5090$ MPa (Fig. 1, c). On the side of the seam in the fusion line, the activation zone with a depth of no more than $40 \mu\text{m}$ with a microhardness of $HV0.5 = 5090 \dots 5490$ MPa in the weld metal and $10 \dots 15 \mu\text{m}$ in the direction of AISI 1010 (in the form of grooves) with $HV0.5 = 4410$ MPa is observed.

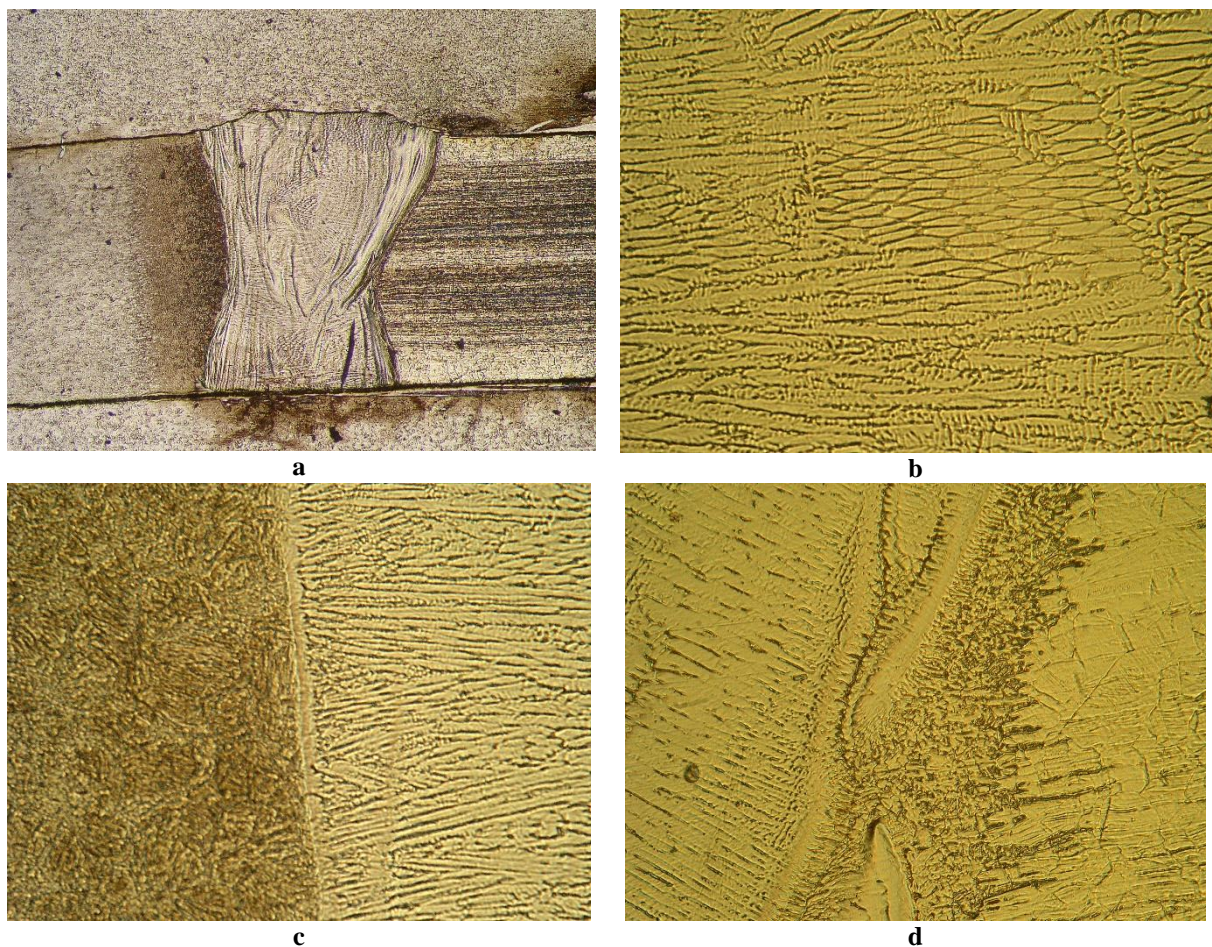


Fig. 1. The structure of the weld of sample No. 1 from AISI 304 stainless steel with 1.5 mm thick AISI 1010 carbon steel:

a – general view $\times 37$; b – seam structure in the central zone $\times 500$; c – structure in the fusion line with AISI 1010 $\times 500$; d – structure in the fusion line with AISI 304 $\times 500$.

On the side of AISI 1010, a heat affected zone (HAZ) is observed, where in the I (coarse-grained) section a bainite structure with a grain size for upper bainite (BU) of $25 \dots 60 \mu\text{m}$ with $HV0.5(BU) = 3410$ MPa and lower bainite (BL) $D_3 = 25 \dots 40 \mu\text{m}$ with $HV0.5(BL) = 3620$ MPa. A ferrite component is also present in the form of rims (with an average thickness of $10 \mu\text{m}$) and equiaxed grains (up to $20 \mu\text{m}$ in size). In the II (normalization) section, the bainite structure size drops to that of $10 \dots 35 \mu\text{m}$, while the microhardness lowers to $HV0.5(B) = 2570$ MPa. There amount of the ferrite component is increased, with an average grain size of $5 \dots 20 \mu\text{m}$. In the III (incomplete recrystallization) section a finely dispersed structure with a grain size of up

to 10 μm and $\text{HV}_{0.5} = 1830\text{...}2070$ MPa is observed. In the IV (recrystallization) section, grain coarsening occurs (up to $h \times l = 12 \times 40$ μm) and the microhardness decreases to $\text{HV}_{0.5} = 1770\text{...}1800$ MPa. The main AISI 1010 metal consists mainly of both elongated (size $h \times l = 10 \times 35$ μm) and equiaxed ($D_3 = 5\text{...}35$ μm) ferrite grains with $\text{HV}_{0.5} = 1550\text{...}1740$ MPa microhardness. A crack with a length of up to 100 μm is observed at the fusion line with AISI 1010 (Fig. 2).

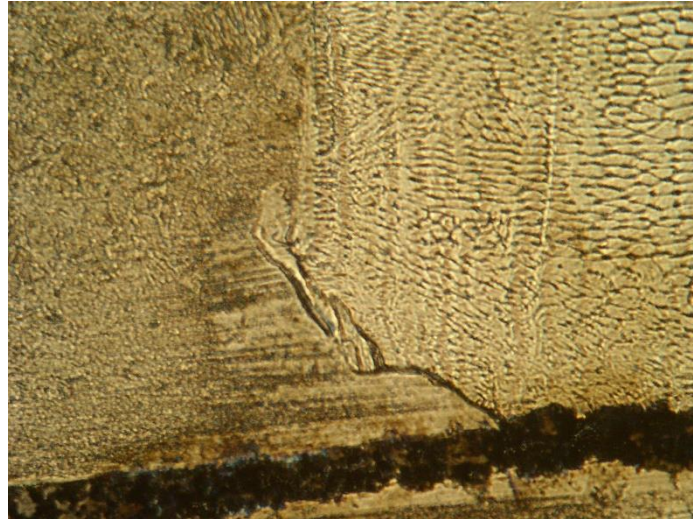


Fig. 2. The structure at the place of crack formation at the fusion line of sample No. 1: welded joint of stainless steel AISI 304 (1.5 mm thick) and carbon steel AISI 1010 (1.5 mm thick) $\times 500$.

Near the fusion line of the seam with AISI 304 stainless steel, activation zones are observed both on the side of the seam metal (with up to a depth of 250 μm) with $\text{HV}_{0.5} = 5270\text{...}5490$ MPa microhardness, and on the side of stainless steel (depth up to 125 μm) with $\text{HV}_{0.5} = 2570\text{...}3210$ MPa (Fig. 1, d). The size of the grain on the side of the stainless steel in the fusion line has the size $h \times l = 25 \times 45$ μm , with microhardness $\text{HV}_{0.5} = 2440\text{...}2810$ MPa. At the same time, in the main metal, are minor changes in both grain size ($h \times l = 20 \times 30$ μm) and microhardness $\text{HV}_{0.5} = 2420\text{...}2630$ MPa were observed.

At the transition of the fusion line in the case of the transition from AISI 304 to the weld metal, a 2-fold change in the concentration of chemical elements (Cr, Ni) and these processes extend to a depth of 20 microns in stainless steel and up to 10 microns in the seam was observed (Fig. 3). At the same time, a sharper change in the concentration of chemical elements (Fe, Cr, Ni) on the side of the seam at a depth of up to 10 microns, and on the side of AISI 1010 up to 5 microns (Fig.4) was observed from the side of the fusion line of AISI 1010 and the weld metal. Channeling of Cr and Ni were also observed in the fusion line of the weld metal with AISI 1010, where the concentration of these elements increased nearly twofold.

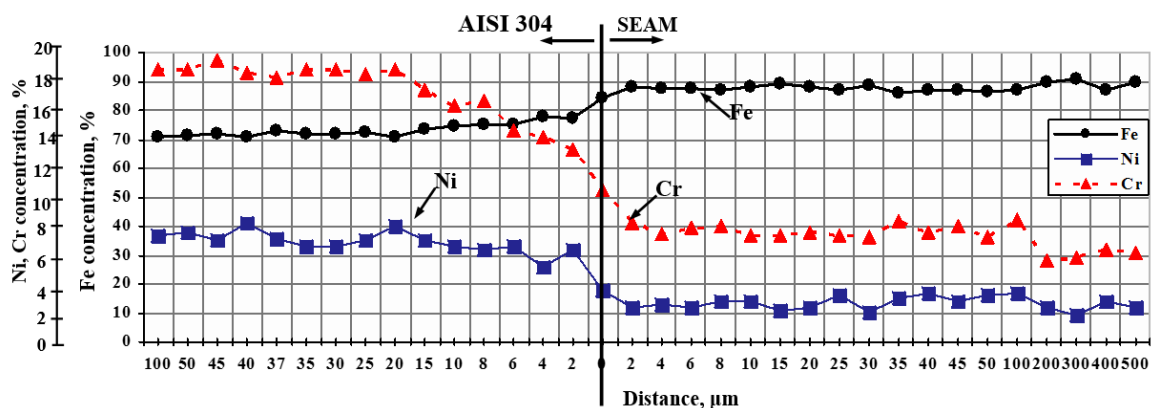


Fig. 3. Distribution of nickel, chromium, and iron at the fusion line of the weld seam with AISI 304 steel of sample No.1 (joint of 1.5 mm thick stainless steel AISI 304 with 1.5 mm thick AISI 1010 carbon steel).

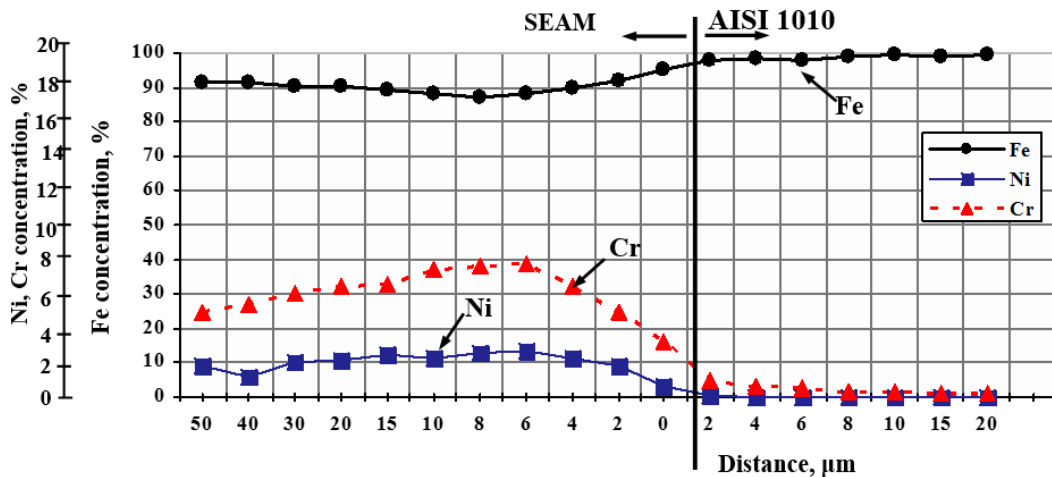


Fig. 4. Distribution of nickel, chromium and iron near and at the fusion line of the weld seam with the AISI 1010 of sample No.1 (joint of 1.5 mm thick stainless steel AISI 304 with 1.5 mm thick AISI 1010 carbon steel).

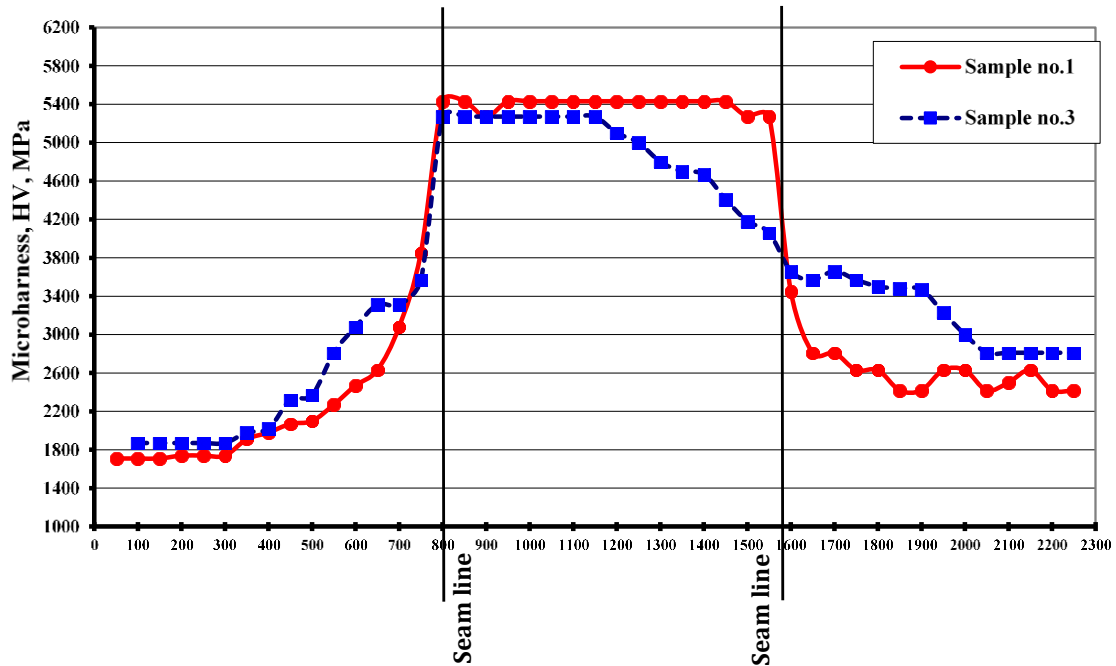


Fig. 5. Graphic representation of the integral distribution of microhardness for samples No.1 and No.3.

As per sample No. 3, which was welded with an offset of 0.7 mm from the joint line to the side of AISI 304 steel, the weld metal has a crystalline structure with the crystallite size $h \times l$ from $5 \times 30 \mu\text{m}$ to $10 \times 65 \mu\text{m}$ (which is, on average, up to 10% smaller compared to the size of the crystallites in the weld metal of sample No. 1) with an average microhardness of $HV_{0.5} = 5270 \text{ MPa}$, which is up to 5% lower compared to the weld metal of sample No. 1 (Fig. 5).

In the fusion line with AISI 1010 (Fig. 6), the zone of activation in the weld metal in sample No. 3 extends to a depth of $140 \mu\text{m}$ on average with microhardness $HV_{0.5} = 5270 \dots 5430 \text{ MPa}$, and in the direction of AISI 1010 – up to to $25 \mu\text{m}$ with $HV_{0.5} = 6180 \dots 6610 \text{ MPa}$ (also in the channeling form). The activation zone in sample No. 3 is 3 times wider compared to sample No. 1, with greater hardness in both AISI 1010 and the weld metal.

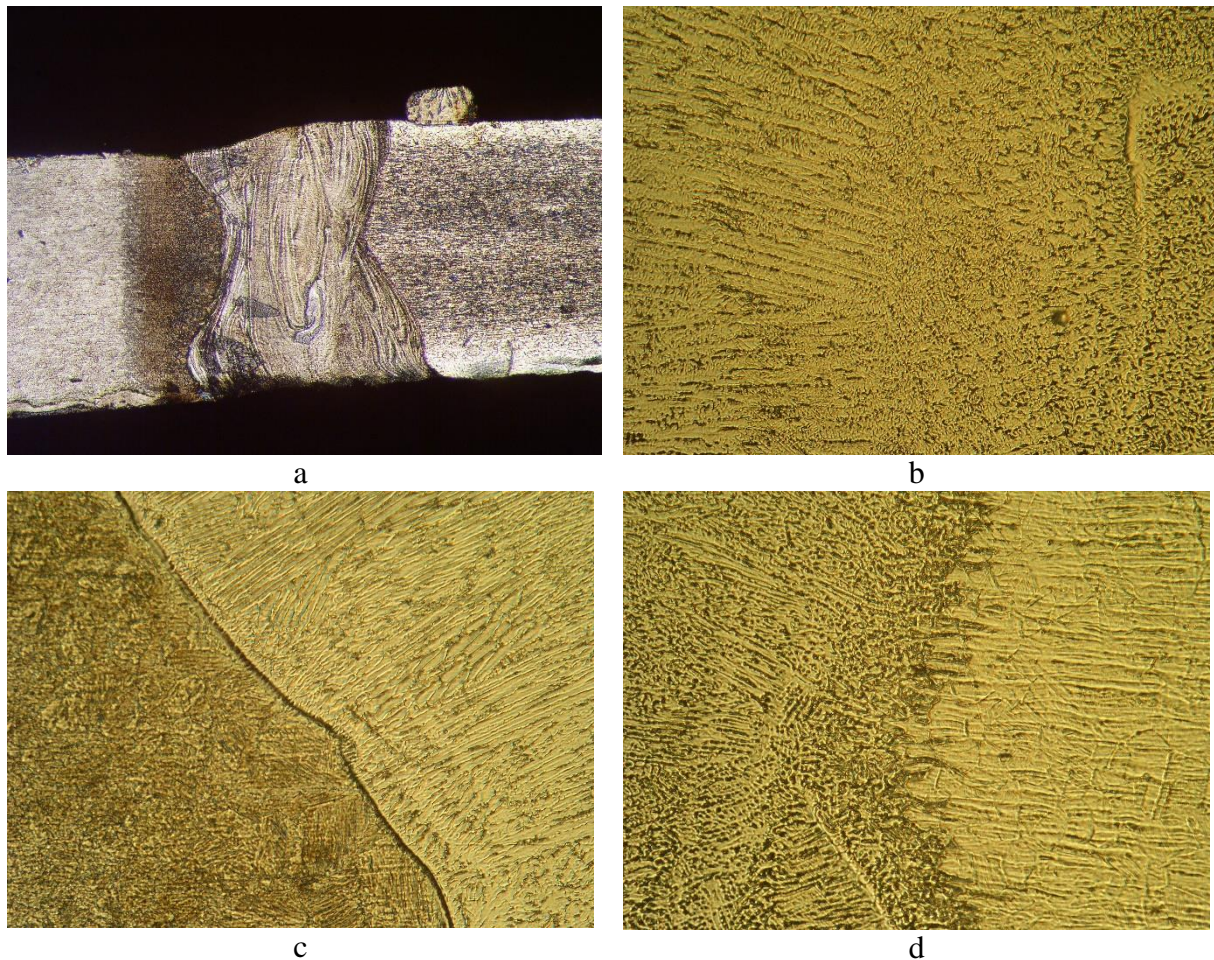


Fig. 6. The structure of the weld of sample No. 3 made of high-chromium stainless steel (1.5 mm thick AISI 304) with carbon steel (1.5 mm thick AISI 1010): a – general view $\times 37$; b – seam structure in the central zone $\times 500$; c – structure in the fusion line with AISI 1010 $\times 500$; d – structure in the fusion line with AISI 304 $\times 500$.

On the AISI 1010 side, the structure of the HAZ practically corresponds to the structure observed in sample No. 1 in all sections of the HAZ. In the I (coarse-grained) section, the bainite structure with a grain size for the upper bainite (BU) of $25\text{...}50\ \mu\text{m}$ with $\text{HV}0.5(\text{BU}) = 3860\ \text{MPa}$ and the lower bainite with a grain size (BL) $D_3 = 25\text{...}40\ \mu\text{m}$ with $\text{HV}0.5(\text{BL}) = 4070\ \text{MPa}$. A ferrite component is also present in the form of rims, $10\ \mu\text{m}$ thick on average.

Compared to sample No. 1, the structure in the large grain zone of sample No. 3 is finer for both BV and BN (up to 10%), and an increase in microhardness by 12% was also recorded. In the II (normalization) section, the bainite structure is diminished to the $10\text{...}30\ \mu\text{m}$ size with $\text{HV}0.5(\text{B}) = 2770\ \text{MPa}$; the observed amount of ferrite component increased. Compared to sample No. 1, in the II zone of the sample No. 3's Heat-Affected Zone, the structure is smaller by 14% (in its relative bainite grain size), while the microhardness increases by 7%. In the III section, a finely dispersed structure with a grain size of up to $10\ \mu\text{m}$ and $\text{HV}0.5 = 2320\ \text{MPa}$ is observed. In the IV (recrystallization) area, the grain size $h \times l$ changes in the range of $5 \times 15\ \mu\text{m}$ to $15 \times 25\ \mu\text{m}$, which is almost 2 times smaller in comparison to the corresponding grain in sample No. 1. Microhardness in this zone is equal to $\text{HV}0.5 = 1830\text{...}1980\ \text{MPa}$, which is up to 10% higher compared to sample No. 1.

Tensile tests of butt-welded joints of AISI 1010 carbon steel and AISI 304 stainless steel were carried out in accordance with GOST 6996-66 "Welded joints. Methods of determining mechanical properties" on the universal servo-hydraulic machine "MTS-318.25" (USA) with a maximum force of 250 kN under normal conditions ($t=20\ ^\circ\text{C}$). The gripper movement speed was equal to $0.17\ \text{mm/s}$. Over the course of the tests, the experimental values of the temporary rupture resistance $426\text{...}446\ \text{MPa}$ were obtained. All welded joints collapsed on the side of AISI 1010 on its base metal at a distance of $15\text{...}25\ \text{mm}$ from the seam and HAZ.

IV. CONCLUSION

During the study of the structure and mechanical characteristics of welded joints made of stainless steel AISI 304 and AISI 1010 carbon steel, it was established that optimal (from the standpoint of structure formation, mechanical characteristics, formation of the geometry of the seam and the absence of defects in the form of cracks, underwelds and burns) welded joints are formed when using such technological techniques as:

1. welding with a shift of a sharply focused laser beam relative to the joint line to the side of a high-chromium steel sample;
2. using gas protection for the welding/melting bath, as well as for the cooling weld metal.

REFERENCES

- [1]. Li, Z., Yu, G., He, X., Tian, C., Li, S., and Li, H. [2022] "Probing thermocapillary convection and multisolute dilution in laser welding of dissimilar miscible metals" *International Journal of Thermal Sciences*, Vol. 172: id.107242.
- [2]. Ai, Y., Liu, X., Huang, Y., and Yu, L. [2021] "Investigation of dissimilar fiber laser welding of low carbon steel and stainless steel by numerical simulation" *Journal of Laser Applications*, Vol. 33, Issue 1: id.012046.
- [3]. Shi, Y., Wu, S., Liao, H., and Wang, X. [2020] "Microstructure and mechanical properties of CLF-1/316 L steel dissimilar joints welded with fiber laser welding" *Journal of Manufacturing Processes*, Vol. 54: pp.318-327.
- [4]. Shi, H. C., Shi, L. B., Ding, H. H., Wang, W. J., Jiang, W. J., Guo, J., and Liu, Q. Y. [2019] "Influence of laser strengthening techniques on anti-wear and anti-fatigue properties of rail welding joint" *Engineering Failure Analysis*, Vol. 101: pp.72-85.
- [5]. Chen, H. C., Ng, F. L., and Du, Z. [2019] "Hybrid laser-TIG welding of dissimilar ferrous steels: 10 mm thick low carbon steel to 304 austenitic stainless steel" *Journal of Manufacturing Processes*, Vol. 47: pp.324-336.
- [6]. Prabakaran, M. P., and Kannan, G. R. [2019] "Optimization of laser welding process parameters in dissimilar joint of stainless steel AISI316/AISI1018 low carbon steel to attain the maximum level of mechanical properties through PWHT" *Optics & Laser Technology*, Vol. 112: pp.314-322.
- [7]. Rajkumar, T., Prabakara, M. P., Arunkumar, G., and GodwinAntony, A. [2020] "Study on the feasibility in welding of low carbon steel and austenitic stainless steel joint using CO₂ laser welding process and analysis of its metallurgical and mechanical properties" *Wutan Huatan Jisuan Jishu*, Vol. 106, Issue 5: pp.471-476.
- [8]. Pańcikiewicz, K., Świerczyńska, A., Hućko, P., and Tumidajewicz, M. [2020] "Laser dissimilar welding of AISI 430F and AISI 304 stainless steels" *Materials*, Vol. 13, Issue 20: id.4540.
- [9]. Pankaj, P., Tiwari, A., Bhadra, R., and Biswas, P. [2019] "Experimental investigation on CO₂ laser butt welding of AISI 304 stainless steel and mild steel thin sheets" *Optics & Laser Technology*, Vol. 119: id.105633.
- [10]. Kumar, P., and Sinha, A. N. [2019] "Effect of average beam power on microstructure and mechanical properties of Nd:YAG laser welding of 304L and st37 steel" *World Journal of Engineering*, Vol. 16, Issue 3: pp.377-388.